Macromolecules

ARTICLE

pubs.acs.org/Macromolecules

Formation of the Inclusion Complex of Helical Syndiotactic Poly(methyl methacrylate) and Polycyclic Aromatic Hydrocarbons

Takehiro Kawauchi,* Mariko Kawauchi, Yuya Kodama, and Tsutomu Takeichi

Department of Environmental and Life Sciences, Toyohashi University of Technology, Tempaku-cho, Toyohashi 441-8580, Japan

Supporting Information

ABSTRACT: We found that polycyclic aromatic hydrocarbons (PAHs) such as pyrene and phenanthrene can be encapsulated in a syndiotactic poly(methyl methacrylate) (st-PMMA) helical cavity, leading to the formation of a crystalline inclusion complex. The inclusion complex of st-PMMA and pyrene (st-PMMA/pyrene) was prepared from the st-PMMA gel formed in a toluene solution of pyrene by drying under vacuum at room temperature for 12 h and at 160 °C for 1 h. The st-PMMA/pyrene inclusion complex containing 19 wt % pyrene showed a characteristic reflection pattern in its X-ray diffractogram and a melting point of 184.4 °C in differential scanning calorimetry experiments. Molecular modeling of the inclusion complex based on the pyrene content indicated that the encapsulated pyrene molecules are closely aligned in the st-PMMA helix. The st-PMMA/pyrene inclusion complex film containing 10 wt % pyrene showed a fluorescence emission because of the formation of a pyrene excimer in the complex, supporting the inference of one-dimensional alignment of the guest molecules in the st-PMMA helical cavity.

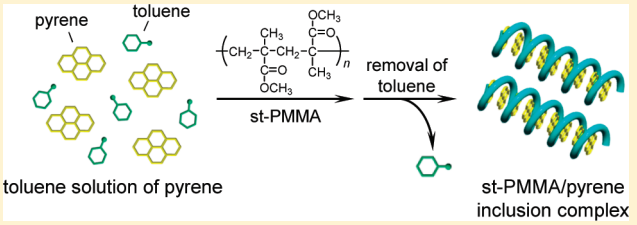

INTRODUCTION

Biological macromolecules such as proteins[1] and DNA[2] form one-handed helical structures that influence their functions in living systems. Inspired by this exquisite helix, many researchers have been motivated to develop fully synthetic helical polymers with controlled helicity. So far, a large number of helical polymers have been synthesized and utilized as chiral materials because of their one-handed helicity.[3] Another important feature resulting from the helical structure is the capability of the polymers to include molecules in the inner helix. Amylose, a natural polysaccharide, is well-known to have a left-handed helical structure in aqueous solutions and to form an inclusion complex with iodine by encapsulating iodine molecules in its helical cavity; this is the so-called "starch−iodide complex".[4] Amylose has also been reported to form inclusion complexes not only with low-molecular-weight organic compounds[5] but also with synthetic polymers.[6] Some natural polysaccharides are now known to be helical host molecules.[4−7] However, inclusion complexes with synthetic helical polymers as the host are still rare.

Syndiotactic poly(methyl methacrylate) (st-PMMA) has been reported to form a thermoreversible physical gel in specific organic solvents such as toluene, in which the st-PMMA chain adopts a helical structure.[8] Kusuyama et al. proposed a 74/4 (= 18.5/1) helical model for the st-PMMA helix induced by organic solvents on the basis of X-ray analysis.[9] The inner diameter of the helix was reported to be ∼1 nm, and hence, solvent molecules are encapsulated in the large cavity. Since the solvent molecules are essential to form the helix, the helical structure is lost once the solvents are completely removed by evaporation in vacuum.[9] Additionally, Saiani and Guenet reported the existence of an irregular double st-PMMA helix in a gel on the basis of small-angle neutron scattering analysis, in which the 74/4 single helix is included in an irregular helix.[10] So far, the unique st-PMMA helical structure has been extensively studied by using IR,[8d,11] NMR,[8a−c,12] fluorescence,[13] X-ray,[9,14] light scattering,[13,14b] rheological,[11,13] and thermal analyses.[10b]

Recently, it was found that fullerenes such as C_{60}, C_{70}, and C_{84} are encapsulated within the helical cavity of st-PMMA to form robust, processable, crystalline inclusion complexes.[15,16] Atomic force microscopy (AFM) and transmission electron microscopy (TEM) studies of a st-PMMA/C_{60} inclusion complex prepared through the Langmuir−Blodgett technique revealed a one-dimensional alignment of the C_{60} molecules in the st-PMMA helix.[15] On the basis of the previous report, we anticipated that the nanospace of the st-PMMA helix would serve as a novel helical host to various guest molecules. In this study, we investigated inclusion complex formation between st-PMMA and polycyclic aromatic hydrocarbons (PAHs), which are used as novel guest molecules. We found that some PAHs such as pyrene and phenanthrene can be encapsulated within the st-PMMA helical cavity, leading to crystalline inclusion complexes with molecular alignment of the guest molecules.

EXPERIMENTAL SECTION

Materials. The st-PMMA was synthesized by the syndiotactic-specific polymerization of MMA in toluene at −95 °C using a typical Ziegler-type catalyst derived from $Al(C_2H_5)_3$ and $TiCl_4$.[17] Isotactic (it-)

Received: February 4, 2011
Revised: March 30, 2011
Published: April 08, 2011

PMMA was prepared by the isotactic-specific anionic polymerization of *tert*-butyl methacrylate in toluene at −78 °C with (1,1-diphenyl-3-methylpentyl)lithium,[18,19] followed by hydrolysis of the pendant esters[19,20] and methylation with diazomethane.[20,21] The number-average molecular weights (M_n), molecular weight distributions (M_w/M_n), and tacticities (*mm*:*mr*:*rr*) are as follows: st-PMMA M_n = 648 000, M_w/M_n = 1.34, and *mm*:*mr*:*rr* = 0:6:94; it-PMMA M_n = 489 000, M_w/M_n = 1.12, and *mm*:*mr*:*rr* = 96:4:0. The M_n and M_w/M_n values were measured by size exclusion chromatography (SEC) in $CHCl_3$ using PMMA standards (Shodex, Tokyo, Japan) for the calibration. The tacticity was determined from the ^{1}H NMR signals due to the α-methyl protons. Toluene, anthracene, phenanthrene, pyrene, and perylene were purchased from Wako Chemicals (Osaka, Japan) and were used as received.

Instruments. NMR spectra were recorded on a Varian Mercury 300 spectrometer (300 MHz for ^{1}H) in $CDCl_3$ using tetramethylsilane (TMS) as the internal standard. Absorption spectra were measured in a 0.1 or 0.2 mm quartz cell by use of a JASCO (Hachioji, Japan) V-500 spectrophotometer. Photoluminescence spectra were recorded on a quartz plate by use of a JASCO FP 6500 spectrofluorometer. Differential scanning calorimetry (DSC) measurements were conducted on a Rigaku (Tokyo, Japan) Thermo Plus 2 DSC-8230 under a nitrogen atmosphere at the heating or cooling rate of 10 °C/min. X-ray measurements were performed with a Rigaku R-AXIS VII system (Rigaku, Tokyo, Japan) equipped with a Rigaku FR-E rotating-anode generator with confocal mirror monochromated Cu Kα radiation (0.154 18 nm) focused through a 0.5 mm pinhole collimator, which was supplied at 45 kV and 45 mA current, equipped with a flat imaging plate having a specimen-to-plate distance of 300 mm. Molecular modeling, molecular mechanics (MM), and molecular dynamics (MD) calculations were performed using Materials Studio software (version 4.0, Accelrys Inc., San Diego, CA).

Preparation of st-PMMA/Pyrene Inclusion Complex Film. A typical experimental procedure is as follows. 10 mg of st-PMMA was dissolved in toluene (1 mL) containing 2.5 mg of pyrene at 110 °C. After the solution was cooled to room temperature, the solution gelled within a few minutes. The st-PMMA/pyrene inclusion complex film was obtained by evaporating the solvent under reduced pressure at room temperature for 12 h followed by further drying under vacuum at 160 °C for 1 h. Pyrene may sublime during the drying process, affording film with lower pyrene content than the theoretical content calculated from the feed content. The exact pyrene content was estimated to be 19 wt % on the basis of its ^{1}H NMR spectrum. In the same way, st-PMMA/pyrene inclusion complex films with various pyrene contents were prepared.

Preparation of st-PMMA/Phenanthrene Inclusion Complex Film. The st-PMMA (10 mg) was dissolved in a toluene solution of phenanthrene (2.5 mg/mL, 1 mL) by heating at 110 °C. After cooling to room temperature, the solution gelled within a few minutes. The st-PMMA/phenanthrene inclusion complex film was obtained by drying the gel under vacuum at room temperature for 12 h and at 120 °C for 1 h. The exact phenanthrene and residual toluene contents were estimated to be 19 and 0.5 wt %, respectively, by ^{1}H NMR analysis.

Molecular Modeling of st-PMMA/Pyrene Inclusion Complex. The geometrical parameters of the reported st-PMMA helix were referred for the construction of an initial 74/4 st-PMMA helix model.[9,15] Based on the X-ray diffraction (XRD) results for st-PMMA/solvent inclusion complexes,[9] the unit height and unit twist of the st-PMMA helix were calculated to be 0.4784 Å and 19.459°, respectively. The bond lengths and bond angles of the st-PMMA main chain were set to 1.54 Å and 109.5°, respectively. According to Miyazawa's equation,[22] the two dihedral angles were then calculated to be −127.92° and 132.96°. The side-chain conformations were assumed to take *trans* and *cis* conformations to the α-methyl group, based on the IR analysis by Tretinnikov et al.[23] The initial model was optimized by using MM calculations with COMPASS force field.[24] Pyrene molecules were manually inserted into the optimized st-PMMA helix so as to form a st-PMMA/pyrene inclusion complex, in which the distance between the encapsulated pyrene molecules was kept constant at 4.12 Å. This spacing is required to satisfy the maximum pyrene content of 19 wt % determined by the DSC analysis. Optimization of the st-PMMA helix was then carried out by MM calculations with the COMPASS force field under the condition that the coordinate of pyrene molecules was fixed. MD simulations were performed for the model using an NTV ensemble.

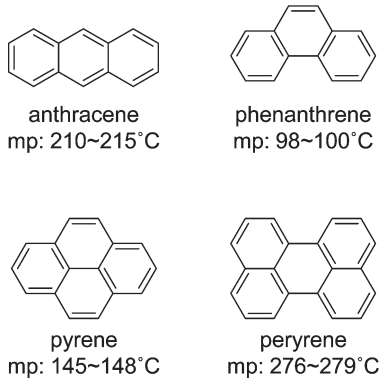

Figure 1. Chemical structures of various PAHs.

RESULTS AND DISCUSSION

Formation of the Inclusion Complex of st-PMMA and Pyrene. The st-PMMA/C_{60} inclusion complex is obtained as a gel by dissolving st-PMMA in a toluene solution of C_{60} by heating at 110 °C and then cooling to room temperature.[15] The st-PMMA/C_{60} condensed gel is precipitated through centrifugation, and the supernatant becomes colorless because the C_{60} molecules are spontaneously encapsulated in the st-PMMA helical cavity. The inclusion complex formation can be monitored quantitatively through UV−vis analysis of the supernatant.

First, we attempted to form inclusion complexes between the st-PMMA gel with toluene and various PAHs, as shown in Figure 1. The st-PMMA was dissolved in a toluene solution of PAH (st-PMMA 10 mg, PAH 2.5 mg, toluene 1 mL) by heating at 110 °C. The solution gelled within a few minutes after cooling to room temperature. The obtained gel was centrifuged and the supernatant was analyzed using UV−vis spectroscopy. However, the concentration of PAH in the supernatant did not change from that of the feed solution, indicating that spontaneous inclusion complex formation with the PAH did not occur in toluene.

In an st-PMMA gel with toluene, the toluene molecules are encapsulated in the st-PMMA helical cavity to form the st-PMMA/toluene inclusion complex. When C_{60} is present in the gel, the st-PMMA/C_{60} inclusion complex is formed.[15] Therefore, it is considered that the affinity of C_{60} for the st-PMMA helix is higher than that of toluene. In the case of PAHs, their affinities for st-PMMA may be equal to or lower than that of toluene; consequently, inclusion complex formation between the PAHs and st-PMMA was not observed in the presence of toluene molecules.

Therefore, we tried to prepare inclusion complexes of st-PMMA and PAHs by removing the toluene molecules from the st-PMMA gel formed in the toluene solution of pyrene. The st-PMMA gel containing pyrene was prepared by dissolving st-PMMA in a toluene solution of pyrene by heating at 110 °C and

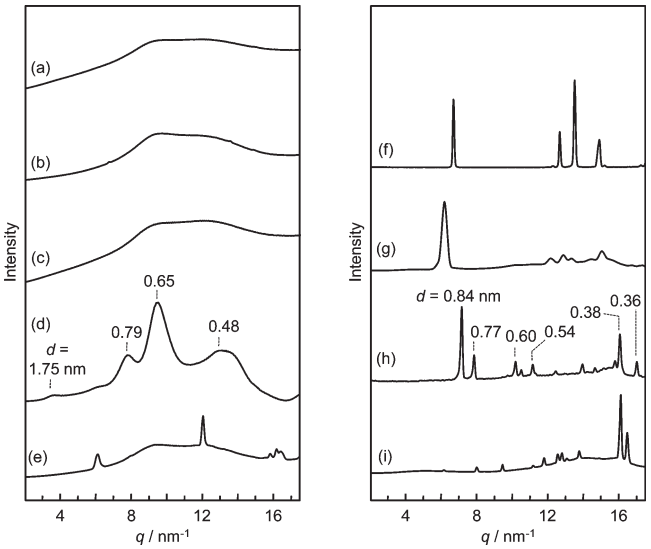

Figure 2. XRD profiles of st-PMMA (a), st-PMMA/anthracene (b), st-PMMA/phenanthrene (c), st-PMMA/pyrene (d), and st-PMMA/perylene (e) films, and anthracene (f), phenanthrene (g), pyrene (h), and perylene (i) powders. The films were prepared by dissolving st-PMMA in a toluene solution of PAH (st-PMMA 10 mg, PAH 2.5 mg, toluene 1 mL) by heating at 110 °C, cooling to room temperature, and drying under vacuum at room temperature for 12 h and then at 160 °C for 1 h.

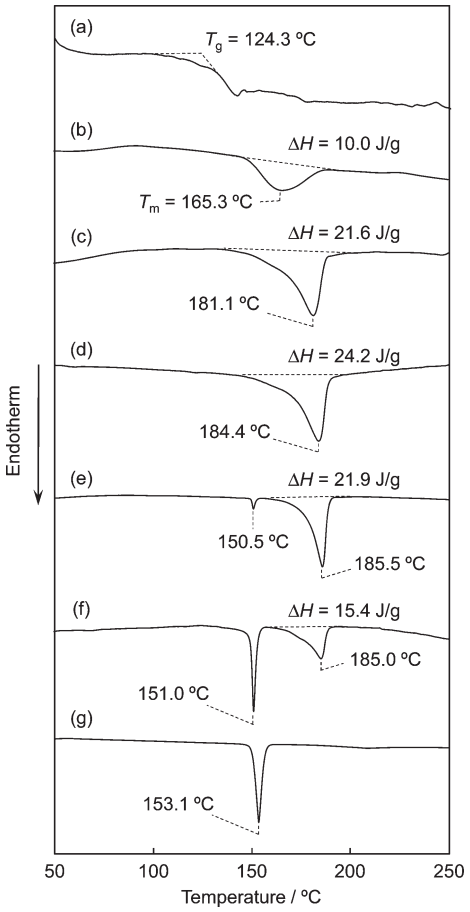

Figure 3. DSC thermograms of the st-PMMA film (a), the st-PMMA/pyrene films containing 10 (b), 14 (c), 19 (d), 26 (e), and 50 wt % (f) pyrene, and pyrene powder (g). The st-PMMA/pyrene films were prepared by dissolving st-PMMA in a toluene solution of pyrene by heating at 110 °C, cooling to room temperature, and drying under vacuum at room temperature for 12 h and then at 160 °C for 1 h. The pyrene contents were determined by ^{1}H NMR analysis.

then cooling to room temperature (st-PMMA 10 mg, pyrene 2.5 mg, toluene 1 mL). Then, a film was obtained by drying the gel under vacuum at room temperature for 12 h; this film contained ∼15 wt % toluene, as estimated from its ^{1}H NMR spectrum. The film was further dried at 160 °C for 1 h to remove the solvent completely. After the drying process, the residual toluene content in the film was estimated to be less than 0.3 wt %. Other st-PMMA films containing different PAHs and a pristine st-PMMA film without PAH were prepared in the same way.

Figure 2 shows the X-ray diffraction (XRD) profiles of the obtained films. The pristine st-PMMA film showed a broad XRD pattern, as is typical for amorphous st-PMMAs (Figure 2a); this indicates that the st-PMMA helical structure was disrupted once the solvent had been completely removed by drying under vacuum at 160 °C for 1 h.[15] Similarly, the st-PMMA films containing anthracene, phenanthrene, and perylene showed broad reflections corresponding to amorphous st-PMMAs, indicating that inclusion complexes were not formed (Figure 2b,c,e). Although sharp reflections are observed in the st-PMMA film containing perylene (e), these correspond to perylene crystals (i). In contrast, the st-PMMA film containing pyrene revealed a characteristic XRD pattern (Figure 2d) that is completely different from those of the pristine st-PMMA film (Figure 2a) and pyrene powder (Figure 2h), but which is similar to the previously reported XRD pattern of the st-PMMA/C_{60} inclusion complex,[15] suggesting the formation of an inclusion complex between st-PMMA and pyrene.

Further evidence for the formation of the st-PMMA/pyrene inclusion complex was found in its characteristic differential scanning calorimetry (DSC) thermogram. St-PMMA/pyrene films with various pyrene contents were prepared and subjected to DSC analysis (Figure 3). The pristine st-PMMA film showed a glass transition temperature (T_g) of 124.3 °C but did not show a melting point (T_m), indicating an amorphous material (Figure 3a). On the other hand, the st-PMMA/pyrene film containing 10 wt % pyrene revealed a T_m at 165.3 °C with an endothermic heat (ΔH) value of 10.0 J/g (Figure 3b) corresponding to the st-PMMA/pyrene inclusion complex, which was essentially different from the melting point of pyrene (T_m = 153.1 °C, Figure 3g). Increasing the pyrene content up to 19 wt % brought about an increase in the crystallinity, a shift in the T_m to over 180 °C, and an increase in ΔH (Figure 3c,d). Further increasing the pyrene content caused ΔH to decrease, while the T_m value of the complex was maintained at ∼185 °C. In addition, we notice the appearance of an endothermic peak at ∼150 °C in Figure 3e,f, corresponding to crystals of pyrene. Parts a and b of Figure 4 show the changes in the T_m and ΔH values, respectively. The ΔH goes through a maximum at 19 wt % pyrene content, whose stoichiometry is 1.2 pyrene molecules per 10 monomeric units of PMMA.[10b] This result suggests that the st-PMMA helical cavity was filled with pyrene molecules at this pyrene content (19 wt %), which is slightly lower than the maximum C_{60} content (23.5 wt %) for the st-PMMA/C_{60} inclusion complex reported previously.[15]

The st-PMMA/pyrene inclusion complex was obtained from the st-PMMA gel formed in the toluene solution of pyrene by drying under vacuum at room temperature for 12 h and at 160 °C

dx.doi.org/10.1021/ma200255m |*Macromolecules* 2011, 44, 3452–3457

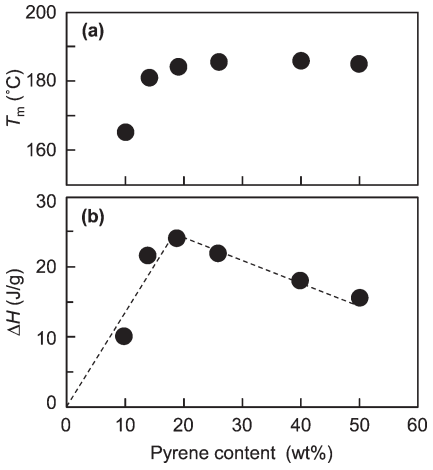

Figure 4. Changes in T_m (a) and ΔH (b) values of blends of st-PMMA and pyrene as a function of the pyrene content.

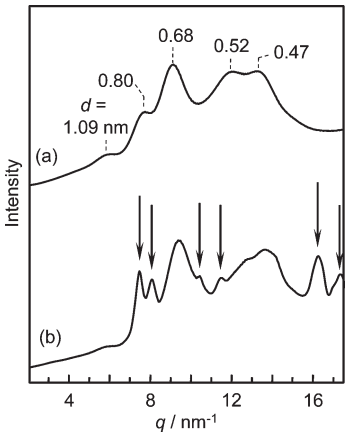

Figure 5. XRD profiles of st-PMMA (a) and st-PMMA/pyrene (b) films containing 18 and 15 wt % toluene, respectively. The st-PMMA film was prepared from the st-PMMA gel with toluene by evaporating the solvent under vacuum at room temperature for 12 h. The st-PMMA/pyrene film was prepared from the st-PMMA gel formed in the toluene solution of pyrene by evaporating the solvent under vacuum at room temperature for 12 h.

for 1 h. We investigated the influence of the drying process on the inclusion complex formation. An st-PMMA film without pyrene was prepared by drying st-PMMA/toluene gel (st-PMMA 10 mg, toluene 1 mL) under vacuum at room temperature for 12 h. The residual toluene content was estimated from its ^{1}H NMR spectrum to be ~18 wt %. XRD of the film revealed a characteristic reflection pattern corresponding to the st-PMMA/solvent inclusion complex (Figure 5a).[14] After drying at 160 °C for 1 h, the film, containing less than 0.3 wt % toluene, showed a broad XRD pattern as mentioned above (Figure 2a) because the induced helical conformation of the st-PMMA chains in the gel formed in toluene was disrupted when the solvent was removed.[9,15]

An st-PMMA/pyrene film containing ~15 wt % toluene was prepared from the st-PMMA gel formed in the toluene solution of pyrene (st-PMMA 10 mg, pyrene 2.5 mg, toluene 1 mL) by drying under vacuum at room temperature for 12 h. Figure 5b shows the XRD profile of this film; the profile shows sharp reflections (indicated by the arrows) corresponding to crystals of pyrene, similar to those observed in Figure 2h. This result indicates that the pyrene molecules were not encapsulated in the st-PMMA helical cavity at this stage. After further drying at 160 °C for 1 h, the sharp reflections due to the pyrene crystals disappeared, and new reflections corresponding to the st-PMMA/pyrene inclusion complex appeared (Figure 2d).

After melting (by heating above T_m), the st-PMMA/pyrene inclusion complex showed a T_g at ~110 °C but did not show an endothermic peak corresponding to T_m, as observed in the DSC measurement during the second heating process (Figure S1b in Supporting Information). Even after annealing at 160 °C for 15 h, T_m was not observed (Figure S1c in Supporting Information). Therefore, it is considered that the prior formation of the st-PMMA helical structure induced by toluene (formation of the st-PMMA/toluene inclusion complex) is essential for the formation of the st-PMMA/pyrene inclusion complex.

On the basis of these results, we propose a possible mechanism for the formation of the inclusion complex of st-PMMA and pyrene from the gel with toluene (Figure 6). In the toluene solution of pyrene, the st-PMMA adopts a helical conformation, which is accompanied by encapsulation of the toluene molecules within the inner helix, resulting in gelation (Figure 6b). After drying the gel under vacuum at room temperature, a mixture of the st-PMMA/toluene inclusion complex and pyrene crystals is obtained (c). By drying the film further at 160 °C under vacuum, the residual toluene molecules evaporate, while the pyrene melts at this temperature (melting point of pyrene: 145−148 °C). Therefore, the molten pyrene is encapsulated in the st-PMMA helical cavity instead of the toluene molecules, affording the st-PMMA/pyrene inclusion complex (d). The drying process at 160 °C is required not only to evaporate the encapsulated toluene molecules but also to melt the guest molecules.

Preparation of st-PMMA/Phenanthrene Inclusion Complex. The drying process strongly affects the formation of the st-PMMA/pyrene inclusion complex from the mixture of the st-PMMA gel with toluene and pyrene. The drying temperature should be higher than the melting point of the guest but lower than that of the inclusion complex. Bearing this finding in mind, we succeeded in preparing an st-PMMA/phenanthrene inclusion complex containing 19 wt % phenanthrene from the st-PMMA gel formed in the toluene solution of phenanthrene (st-PMMA 10 mg, phenanthrene 2.5 mg, toluene 1 mL) by drying under vacuum at 120 °C (the residual toluene content was estimated to be 0.5 wt % by ^{1}H NMR). The film containing st-PMMA and phenanthrene prepared by drying at 160 °C showed an amorphous XRD pattern (Figure 2c), whereas the one prepared by drying at 120 °C showed a characteristic XRD pattern corresponding to the inclusion complex (Figure 7a). The DSC thermogram of the st-PMMA/phenanthrene inclusion complex film also showed an exothermic peak at 123.9 °C corresponding to the melting point of the complex (Figure 7b), thus confirming the formation of the inclusion complex. On the other hand, anthracene and peryrene did not form inclusion complexes even when the drying temperature was varied in the range 120−220 °C, probably because the melting points of anthracene and peryrene are higher than the expected melting points of the st-PMMA inclusion complexes.

Array of Guest Molecules within the st-PMMA Helical Cavity. From the DSC analysis mentioned above (Figures 3 and 4), it was suggested that the st-PMMA/pyrene inclusion complex film containing 19 wt % pyrene had high crystallinity and that the st-PMMA helical cavity was filled with pyrene molecules at this pyrene content. Molecular modeling of the

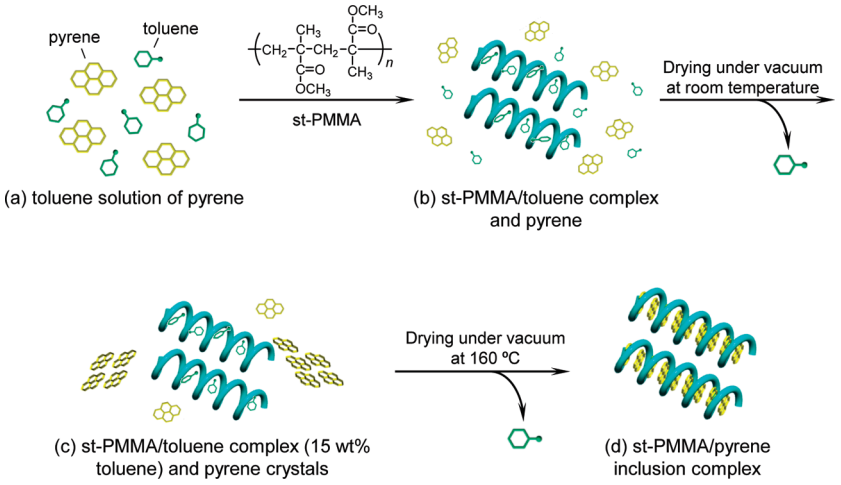

Figure 6. Schematic illustration of a possible mechanism for the formation of the inclusion complex of st-PMMA and pyrene from the toluene gel.

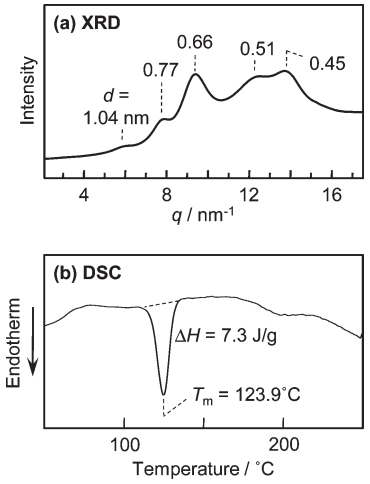

Figure 7. XRD profile (a) and DSC thermogram (b) of the st-PMMA/phenanthrene film prepared from the st-PMMA gel formed in the toluene solution of phenanthrene by drying under vacuum at room temperature for 12 h and at 120 °C for 1 h.

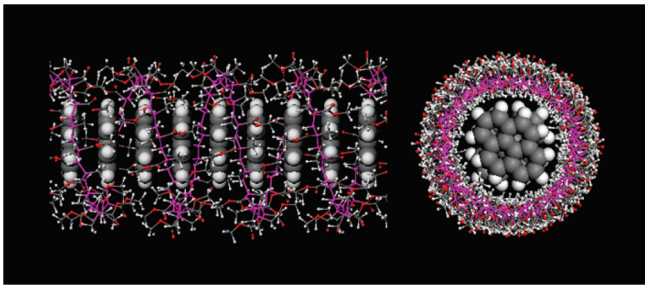

Figure 8. Possible structure of the st-PMMA/pyrene inclusion complex containing 19 wt % pyrene (left: side view; right: top view).

st-PMMA/pyrene inclusion complex was performed in accordance with these results. The st-PMMA 74/4 helix was constructed on the basis of the XRD results of st-PMMA/solvent inclusion complexes reported by Kusuyama et al.[9] Subsequently, pyrene molecules were manually inserted into the helix so as to satisfy the maximum pyrene content of 19 wt % determined by

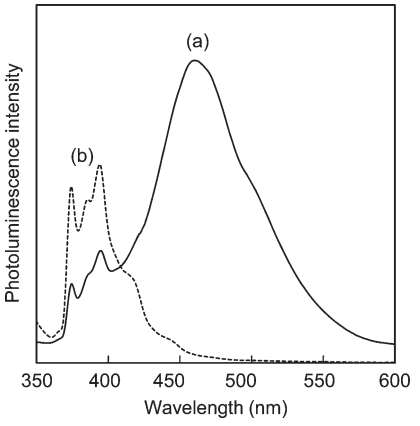

Figure 9. Photoluminescence (excitation wavelength = 337 nm) spectra of st-PMMA/pyrene (a, solid line) and it-PMMA/pyrene (b, dashed line) films. The pyrene content was 10 wt %.

DSC analysis. The st-PMMA helix was then optimized by molecular mechanics (MM) calculations with the COMPASS force field.[24] The model constructed is shown in Figure 8; the pyrene molecules were stacked in the st-PMMA helix and the distance between them was 4.12 Å, suggesting their one-dimensional alignment. Molecular dynamics (MD) simulations of the st-PMMA/pyrene inclusion complex using an NTV ensemble revealed that the encapsulated pyrene molecules remain within the st-PMMA helical cavity even at 400 K for 200 ps (Figure S2 in Supporting Information), which indicates the high thermal stability of the complex.

On the basis of the molecular modeling, it is proposed that the pyrene molecules are encapsulated in the st-PMMA helix to form a regular one-dimensional array. Pyrene is known to form an excited-state dimer (excimer) upon close encounter with another pyrene molecule. Therefore, it was anticipated that the st-PMMA/pyrene inclusion complex might reveal excimer fluorescence properties. Figure 9a shows the photoluminescence spectrum of an st-PMMA/pyrene inclusion complex containing 10 wt % pyrene, formed on a quartz plate. The film revealed a fluorescence emission due to the pyrene excimer at 462 nm, whereas a mixture film of isotactic PMMA (it-PMMA) and pyrene prepared under the same conditions mainly showed a

monomeric fluorescence emission at around 390 nm (Figure 9b). This result supports the conclusion that the encapsulated pyrene molecules in the st-PMMA helical cavity are closely aligned.

In summary, we have found that some PAHs such as pyrene and phenanthrene can be encapsulated in the st-PMMA helical cavity, leading to the formation of crystalline inclusion complexes. In order to form the st-PMMA/PAH inclusion complex, prior formation of the st-PMMA/toluene inclusion complex is essential. The high-temperature drying process conditions are also crucial: the temperature should be higher than the melting point of the guest species but lower than that of the corresponding st-PMMA/PAH inclusion complex. The formation process is quite different from that of the st-PMMA/C_{60} inclusion complex reported previously.[15] The st-PMMA/pyrene inclusion complex film was obtained from the st-PMMA gel formed in the toluene solution of pyrene by drying under vacuum at room temperature for 12 h and at 160 °C for 1 h; the complex formed showed a characteristic XRD reflection pattern and a melting point over 180 °C from DSC measurements. The maximum pyrene content was estimated to be 19 wt % from the DSC analysis. Molecular modeling based on the maximum content implied that the encapsulated pyrene molecules are closely aligned in the st-PMMA helical cavity. The st-PMMA/pyrene inclusion complex film containing 10 wt % pyrene showed a fluorescence emission due to a pyrene excimer formed in the st-PMMA helix, supporting the one-dimensional alignment of the guest molecules. By using the methodology developed here, other molecules may be encapsulated in the st-PMMA helical cavity, which can serve as a one-dimensional host to array the guest molecules. This technique could provide advanced polymeric materials with unique characteristics based on the arrayed guest species.

■ ASSOCIATED CONTENT

Supporting Information. DSC thermograms of the st-PMMA/pyrene film after melting and MD simulations of the st-PMMA/pyrene inclusion complex. This material is available free of charge via the Internet at http://pubs.acs.org.

■ AUTHOR INFORMATION

Corresponding Author
*E-mail: kawauchi@ens.tut.ac.jp.

■ ACKNOWLEDGMENT

We are deeply grateful to Mr. A. Kitaura, Dr. H. Iida, and Professor E. Yashima (Nagoya University) for X-ray measurements and computer simulations. This work was partially supported by Grant-in-Aid for Young Scientists (B) from the Ministry of Education, Culture, Sports, Science, and Technology, Japan.

■ REFERENCES

(1) Pauling, L.; Corey, R. B.; Branson, H. R. *Proc. Natl. Acad. Sci. U.S.A.* **1951**, *37*, 205–210.
(2) Watson, J. D.; Crick, F. H. C. *Nature* **1953**, *171*, 737–738.
(3) For reviews: (a) Okamoto, Y.; Nakano, T. *Chem. Rev.* **1994**, *94*, 349–372. (b) Wulff, G. *Angew. Chem., Int. Ed. Engl.* **1989**, 28–37. (c) Green, M. M.; Peterson, N. C.; Sato, T.; Teramoto, A.; Cook, R.; Lifson, S. *Science* **1995**, *268*, 1860–1866. (d) Okamoto, Y.; Yashima, E. *Angew. Chem., Int. Ed.* **1998**, *37*, 1020–1043. (e) Hill, D. J.; Mio, M. J.; Prince, R. B.; Hughes, T. S.; Moore, J. S. *Chem. Rev.* **2001**, *101*, 3893–4011. (f) Nakano, T.; Okamoto, Y. *Chem. Rev.* **2001**, *101*, 4013–4038. (g) Huc, I. *Eur. J. Org. Chem.* **2004**, *1*, 17–29. (h) Yashima, E.; Maeda, K. *Macromolecules* **2008**, *41*, 3–12. (i) Ikai, T.; Okamoto, Y. *Chem. Rev.* **2009**, *109*, 6077–6101. (j) Kumaki, J.; Sakurai, S.; Yashima, E. *Chem. Soc. Rev.* **2009**, *38*, 737–746. (k) Yashima, E.; Maeda, K.; Iida, H.; Furusho, Y.; Nagai, K. *Chem. Rev.* **2009**, *109*, 6102–6211. (l) Yashima, E. *Polym. J.* **2010**, *42*, 3–16.
(4) Bishop, R.; Dance, I. G. *Top. Curr. Chem.* **1988**, *149*, 137–188.
(5) (a) Hui, Y.; Russell, J. C.; Whitten, D. G. *J. Am. Chem. Soc.* **1983**, *105*, 1374–1376. (b) Kim, O.-K.; Choi, L.-S. *Langmuir* **1994**, *10*, 2842–2846.
(6) (a) Kaneko, Y.; Kadokawa, J. *Chem. Rec.* **2005**, *5*, 36–46. (b) Sanji, T.; Kato, N.; Kato, M.; Tanaka, M. *Angew. Chem., Int. Ed.* **2005**, *44*, 7301–7304. (c) Ikeda, M.; Furusho, Y.; Okoshi, K.; Tanahara, S.; Maeda, K.; Nishino, S.; Mori, T.; Yashima., E. *Angew. Chem., Int. Ed.* **2006**, *45*, 6491–6495.
(7) (a) Li, C.; Numata, M.; Bae, A.-H.; Sakurai, K.; Shinkai, S. *J. Am. Chem. Soc.* **2005**, *127*, 4548–4549. (b) Bae, A.-H.; Numata, M.; Hasegawa, T.; Li, C.; Kaneko, K.; Sakurai, K.; Shinkai, S. *Angew. Chem., Int. Ed.* **2005**, *44*, 2030–2033. (c) Numata, M.; Tamesue, S.; Nagasaki, T.; Sakurai, K.; Shinkai, S. *Chem. Lett.* **2007**, *36*, 668–669. (d) Haraguchi, S.; Numata, M.; Li, C.; Nakano, Y.; Fujiki, M.; Shinkai, S. *Chem. Lett.* **2009**, *38*, 254–255.
(8) (a) Spěváček, J. *J. Polym. Sci., Polym. Phys. Ed.* **1978**, 523–528. (b) Spěváček, J.; Schneider, B. *Polym. Bull.* **1980**, 227–233. (c) Spěváček, J.; Schneider, B.; Bohdanecký, M.; Sikora, A. *J. Polym. Sci., Polym. Phys. Ed.* **1982**, 1623–1632. (d) Spěváček, J.; Schneider, B.; Dybal, J.; Stokr, J.; Baldrian, J.; Pelzbauer, Z. *J. Polym. Sci., Polym. Phys. Ed.* **1984**, 617–635.
(9) (a) Kusuyama, H.; Takase, M.; Higashihara, Y.; Tseng, H.-T.; Chatani, Y.; Tadokoro, H. *Polymer* **1982**, *23*, 1256–1258. (b) Kusuyama, H.; Miyamoto, N.; Chatani, Y.; Tadokoro, H. *Polym. Commun.* **1983**, *24*, 119–122.
(10) (a) Saiani, A.; Guenet, J.-M. *Macromolecules* **1997**, *30*, 966–972. (b) Saiani, A.; Spěváček, J.; Guenet, J.-M. *Macromolecules* **1998**, *31*, 703–710. (c) Saiani, A.; Guenet, J.-M. *Macromolecules* **1999**, *32*, 657–663.
(11) Buyse, K.; Berghmans, H.; Bosco, M.; Paoletti, S. *Macromolecules* **1998**, *31*, 9224–9230.
(12) (a) Spěváček, J.; Schneider, B.; Straka, J. *Macromolecules* **1990**, *23*, 3042–3051. (b) Spěváček, J.; Suchopárek, M. *Macromolecules* **1997**, *30*, 2178–2181.
(13) Berghmans, M.; Thijs, S.; Cornette, M.; Berghmans, H.; De Schryver, F. C. *Macromolecules* **1994**, *27*, 7669–7676.
(14) (a) Könnecke, K.; Rehage, G. *Colloid Polym. Sci.* **1981**, *259*, 1062–1069. (b) Sedláček, B.; Spěváček, J.; Mrkvičková, L.; Stejskal, J.; Horská, J.; Baldrian, J.; Quadrat, O. *Macromolecules* **1984**, *17*, 825–837.
(15) Kawauchi, T.; Kumaki, J.; Kitaura, A.; Okoshi, K.; Kusanagi, H.; Kobayashi, K.; Sugai, T.; Shinohara, H.; Yashima, E. *Angew. Chem., Int. Ed.* **2008**, *47*, 515–519.
(16) (a) Kawauchi, T.; Kitaura, A.; Kumaki, J.; Kusanagi, H.; Yashima, E. *J. Am. Chem. Soc.* **2008**, *130*, 11889–11891. (b) Kawauchi, M.; Kawauchi, T.; Takeichi, T. *Macromolecules* **2009**, *42*, 6136–6140. (c) Kawauchi, T.; Kitaura, A.; Kawauchi, M.; Takeichi, T.; Kumaki, J.; Iida, H.; Yashima, H. *J. Am. Chem. Soc.* **2010**, *132*, 12191–12193. (d) Kitaura, A.; Iida, H.; Kawauchi, T.; Yashima, E. *Chem. Lett.* **2011**, *40*, 28–30.
(17) Abe, H.; Imai, K.; Matsumoto, M. *J. Polym. Sci., Part C* **1968**, *23*, 469–485.
(18) Varshney, S. K.; Gao, Z.; Zhong, X.-F.; Eisenberg, A. *Macromolecules* **1994**, *27*, 1076–1082.
(19) Kawauchi, T.; Kumaki, J.; Yashima, E. *J. Am. Chem. Soc.* **2005**, *127*, 9950–9951.
(20) Kitayama, T.; He, S.; Hironaka, Y.; Iijima, T.; Hatada, K. *Polym. J.* **1995**, *27*, 314–318.
(21) Katchalsky, A.; Eisenberg, H. *J. Polym. Sci.* **1951**, *6*, 145–154.
(22) Miyazawa, T. *J. Polym. Sci.* **1961**, *55*, 215–231.
(23) Tretinnikov, O. N.; Ohta, K. *Macromolecules* **2002**, *35*, 7343–7353.
(24) Sun, H. *J. Phys. Chem. B* **1998**, *102*, 7338–7364.